# Structural Characterization of Folded and Unfolded States of an SH3 Domain in Equilibrium in Aqueous Buffer†

Ouwen Zhang‡,§ and Julie D. Forman-Kay*,‡

*Biochemistry Research Division, Hospital for Sick Children and Department of Biochemistry, University of Toronto, Toronto, Ontario, M5G 1X8 Canada, and Department of Chemistry, University of Toronto, Toronto, Ontario, M5S 1A1 Canada*

*Received December 28, 1994; Revised Manuscript Received March 10, 1995*⊗

ABSTRACT: The isolated N-terminal Src homology 3 (SH3) domain of *Drosophila* drk exists in equilibrium between folded and unfolded states in aqueous buffer near neutral pH. Nuclear magnetic resonance spectra recorded on both states simultaneously exhibit an approximate 1:1 ratio of protein conformations. The folded form is similar to other known SH3 structures, especially the N-terminal SH3 domain of the mammalian homologue GRB2. A stretch of sequential amide−amide nuclear Overhauser effect cross-peaks for resonances of the unfolded state is observed in a region corresponding to β-strands in the folded state. The results suggest that turn-like conformations may be preferentially sampled in the folding pathway for this predominantly β-structured SH3 domain. In addition, a stable turn at Leu-28 is observed in the unfolded but not in the folded state. Comparison of this unfolded form with a denatured state in 2 M guanidine hydrochloride shows that, while both are highly disordered, these states are not identical and more residual structure is present under nondenaturing conditions.

The presence of non-native structures on the folding pathway for a protein is an issue of current interest (Weissman & Kim, 1992; Creighton, 1992). Since folding of proteins can be in the millisecond time scale, structural characterization of intermediates is difficult (Kuwajima et al., 1988). Intermediates can be trapped by using pulse hydrogen exchange methods (Udgaonkar & Baldwin, 1988; Roder et al., 1988). Indirect information can be obtained by the study of partially structured equilibrium "intermediate" states. These include "molten-globules" observed in low pH or mildly denaturing conditions (Ptitsyn et al., 1990), those derived from fragments or mutants of proteins (Flanagan et al., 1992; Lim et al., 1992), and unfolded forms containing residual structure (Shortle, 1993). Due to the stability of these equilibrium states over periods long enough to allow structural characterization, they can be studied as models for kinetic intermediates in folding. Nuclear magnetic resonance (NMR)[1] spectroscopy is a powerful tool for the elucidation of structure in these equilibrium "intermediate" and unfolded states of proteins. A stretch of seven residues of the urea-denatured 434-repressor was found to maintain a stable native-like hydrophobic cluster using NMR approaches (Neri et al., 1992). Structural characterization of unfolded states of FK506 binding protein (FKBP), however, revealed some differences in the secondary structure of the C-terminus of the molecule from that found in the folded state (Logan et al., 1994).

As we have previously reported (Zhang et al., 1994; Farrow et al., 1994, 1995), the isolated N-terminal Src homology 3 (SH3) domain of the *Drosophila* signal transduction protein drk is in equilibrium between folded and unfolded states in aqueous buffer conditions. This system presents an ideal case for the comparison of residual structure in an unfolded state under nondenaturing conditions with the folded structure under the same conditions. This comparison has enabled us to address the issues of non-native residual structure and the sensitivity of structure in unfolded states to solution conditions. It is of interest to note that a similar equilibrium between folded and unfolded states of the N-terminal SH3 domain of GRB2 at pH 3.5 in water was also recently reported (Goudreau et al., 1994).

The *Drosophila* protein drk is a modular 23 kDa protein containing a central Src homology 2 (SH2) domain surrounded by two SH3 domains (Olivier et al., 1993; Simon et al., 1993). SH3 domains, 50−70 residues in length, are found in a number of proteins having distinct activities involved in signal transduction and cellular localization (Koch et al., 1991; Bar-Sagi et al., 1993). Drk and its *C. elegans* and mammalian homologues Sem-5 and GRB2, respectively, mediate interactions between receptor tyrosine kinases and *ras* G-proteins by the binding of their SH3 domains to proline-rich, hydrophobic regions of guanine nucleotide exchange proteins such as Sos (Musacchio et al., 1992a; Cicchetti et al., 1992; Pawson & Gish, 1992). Isolated SH3 domains from signalling proteins, including spectrin, cytoplasmic tyrosine kinases, and GRB2, fold independently into functional forms which retain native

† This work was supported by grants to J.D.F.-K. from the National Cancer Institute of Canada with funds from the Canadian Cancer Society and from the Medical Research Council of Canada. O.Z. is the recipient of an Open Fellowship from the University of Toronto.

‡ Hospital for Sick Children and Department of Biochemistry, University of Toronto.

§ Department of Chemistry, University of Toronto.

⊗ Abstract published in *Advance ACS Abstracts,* May 1, 1995.

[1] Abbreviations: NMR, nuclear magnetic resonance; FKBP, FK506 binding protein; SH3, Src homology 3 domain; SH2, Src homology 2 domain; drkN SH3, N-terminal SH3 domain of drk; Gdn, guanidine hydrochloride; HSQC, heteronuclear single quantum coherence spectroscopy; NOE, nuclear Overhauser effect; NOESY, NOE spectroscopy; TOCSY, total correlation spectroscopy; $F_{exch}$, folded state of the drkN SH3 domain existing in equilibrium with the unfolded state in low ionic strength aqueous buffer; $F_S$, fully stabilized folded state of the drkN SH3 domain in 0.4 M $Na_2SO_4$; $U_{exch}$, unfolded state of the drkN SH3 domain existing in equilibrium with the folded state in low ionic strength aqueous buffer; $U_{Gdn}$, denatured state of the drkN SH3 domain in 2 M Gdn.

0006-2960/95/0434-6784$09.00/0 

binding characteristics. Structural studies of these isolated SH3 domains have revealed a $\beta$-barrel composed of two orthogonal three-stranded $\beta$-sheets with an associated irregular two-stranded sheet (Musacchio et al., 1992b; Yu et al., 1992; Kohda et al., 1993; Booker et al., 1993; Koyama et al., 1993; Noble et al., 1993; Yang et al., 1994; Borchert et al., 1994; Kohda et al., 1994). Structures of complexes of isolated SH3 domains with polyproline helical peptides derived from target binding proteins have also been determined for several SH3 domains (Musacchio et al., 1994; Yu et al., 1994; Feng et al., 1994), including a number of independent structures of Sos-derived peptide complexes of the N-terminal SH3 domain of GRB2 (Wittekind et al., 1994; Teresawa et al., 1994; Goudreau et al., 1994).

In this work, we present structural characterization of folded and unfolded states of the N-terminal SH3 domain of drk in aqueous buffer conditions. The two states are in slow exchange on the NMR time scale in 50 mM sodium phosphate, pH 6.0−7.5 and 23−37 °C. These conditions have been used to study many native states of proteins and are not typically destabilizing of native protein structure (Pace, 1975). Heteronuclear NMR experiments were utilized to assign the backbone proton and $^{15}N$ resonances (Zhang et al., 1994) of the folded and unfolded states of the SH3 domain under these conditions and to allow characterization of the structure of both forms. In addition, we present a structural comparison of these states with a fully stabilized folded form in high salt and a denatured form in guanidine hydrochloride (Gdn).

## EXPERIMENTAL PROCEDURES

*Sample Preparation.* A gene fragment coding for the isolated N-terminal SH3 domain of drk (drkN SH3), containing residues 1 through 59 of the original drk clone (Olivier et al., 1993), was inserted into a pET-11d plasmid vector under the control of the T7 promoter. The construct includes 59 residues up to the highly conserved tryptophan residue (Trp-60) which is part of the hydrophobic core of SH2 domains [reviewed in Kuriyan and Cowburn (1993)] and contains all sequences required for the formation of the SH3 tertiary fold, based on homology with other isolated SH3 domains whose structures are known. Isotopic labeling with $^{15}N$ was utilized in order to exploit the chemical shift dispersion of $^{15}N$ in unfolded states, similar to that of folded proteins, for resolution of the clustered amide protons of the unfolded state which resonate between 8 and 8.5 ppm. The plasmid was transfected into *Escherichia coli* BL21 cells, and expression of $^{15}N$-labeled protein was induced for 2 h at $OD_{600}$ of 0.6−0.8 by addition of 250 mg/L IPTG to bacterial growths at 37 °C in M9 minimal media, supplemented with 0.3% glucose and 0.1% $^{15}NH_4Cl$ (99% enriched). The M9 was also supplemented with 100 mg/L ampicillin, 10 mg/L biotin, 10 mg/L thiamin, and 1 mM each $MgSO_4$ and $CaCl_2$. Cells were lysed by sonication in 50 mM L-histidine, 2 mM EDTA, 5 mM benzamidine, and 7 mM $\beta$-mercaptoethanol. The drkN SH3 domain was purified on a DEAE-Sephacel ion-exchange column with a linear gradient of NaCl (0−1 M) followed by an S-100 gel filtration column in 0.5 M NaCl. Purity was estimated at over 99% from SDS−PAGE analysis. The identity of the protein was confirmed by N-terminal amino acid sequencing on a Porton Gas-phase Microseqencer and by amino acid analysis. In addition, the molecular weight observed from mass spectroscopy was identical to the calculated value. Yields of approximately 3 mg/L culture were obtained.

NMR samples of the equilibrium mixture of folded and unfolded states of the drkN SH3 domain contained 0.5−1.0 mM protein in 50 mM sodium phosphate, pH 6.0, 90% $H_2O$/10% $D_2O$. Addition of 50 mM $Na_2SO_4$ to some of these samples was used to help prevent aggregation of the SH3 domain over long periods of time at room temperature or above. Samples of fully stabilized folded and fully denatured drkN SH3 domain were prepared by adding $Na_2SO_4$ to 0.4 M concentration and Gdn to 2 M concentration, respectively, to the protein in 50 mM sodium phosphate, pH 6.0, 90% $H_2O$/10% $D_2O$. The pH of the 2 M Gdn sample was then adjusted to 6.0 with small amounts of NaOH. Samples for the Gdn, $Na_2SO_4$, and pH titrations were prepared as described in Table 1.

*NMR Spectroscopy.* NMR experiments were performed on Varian Unity 500 MHz spectrometers equipped with actively shielded Z-gradient probes and gradient amplifier units. Data were processed and analyzed on SUN SparcStations using Varian VNMR, nmrPipe/nmrDraw (Delaglio, 1993), and PIPP (Garrett et al., 1991) software. A version of the HMQC-J experiment (Kay & Bax, 1990) including pulsed field gradients for water suppression was recorded to measure $^3J_{HN\alpha}$ coupling constants and was processed and analyzed as described previously (Forman-Kay et al., 1990). A modified sensitivity enhanced gradient HSQC experiment (Kay et al., 1992) was utilized, incorporating additional pulsed field gradients for artifact suppression. In order to assign the resonances and characterize the structures of both folded and unfolded states of the drkN SH3 domain, 3D $^{15}N$-edited NOESY-HSQC (150 ms) and TOCSY-HSQC spectra (55 ms) were recorded on both forms simultaneously, using a 1 mM sample in 50 mM sodium phosphate, pH 6.0 and 30 °C, conditions which yield an approximately 1:1 ratio between the two states. Pulsed field gradients were employed, and the enhanced sensitivity (Kay et al., 1992) gradient HSQC approach was incorporated into the 3D $^{15}N$-edited NOESY and TOCSY experiments (Zhang et al., 1994). The large chemical shift dispersions for $^1H$ and $^{15}N$ in the folded state and for $^{15}N$ in this unfolded state allow almost complete resolution of amides from these two forms (Figure 1A). We also recorded 3D $^{15}N$-edited NOESY and TOCSY spectra on a sample of the fully stabilized folded state of the drkN SH3 domain in 0.4 M $Na_2SO_4$ in order to enable comparison of the folded states in low and high salt and on a sample of the denatured drkN SH3 domain in 2 M Gdn in order to compare the two unfolded states. Assignments have been published elsewhere (Zhang et al., 1994). Since the rate of amide proton exchange with solvent in unfolded states is greater, on average, than in native states (Englander & Kallenbach, 1984; Rashin, 1987), experiments which minimize the saturation of the water were utilized in all cases. Results of relaxation experiments on the drkN SH3 domain described in Farrow et al. (1994, 1995) were utilized in the interpretation of the data.

## RESULTS AND DISCUSSION

*Conformational Exchange.* The isolated N-terminal SH3 of drk was expected to form a stable folded structure in solution, in a similar fashion to other isolated SH3 domains and other isolated domains of modular proteins. However, twice the number of expected peaks for a protein of 59

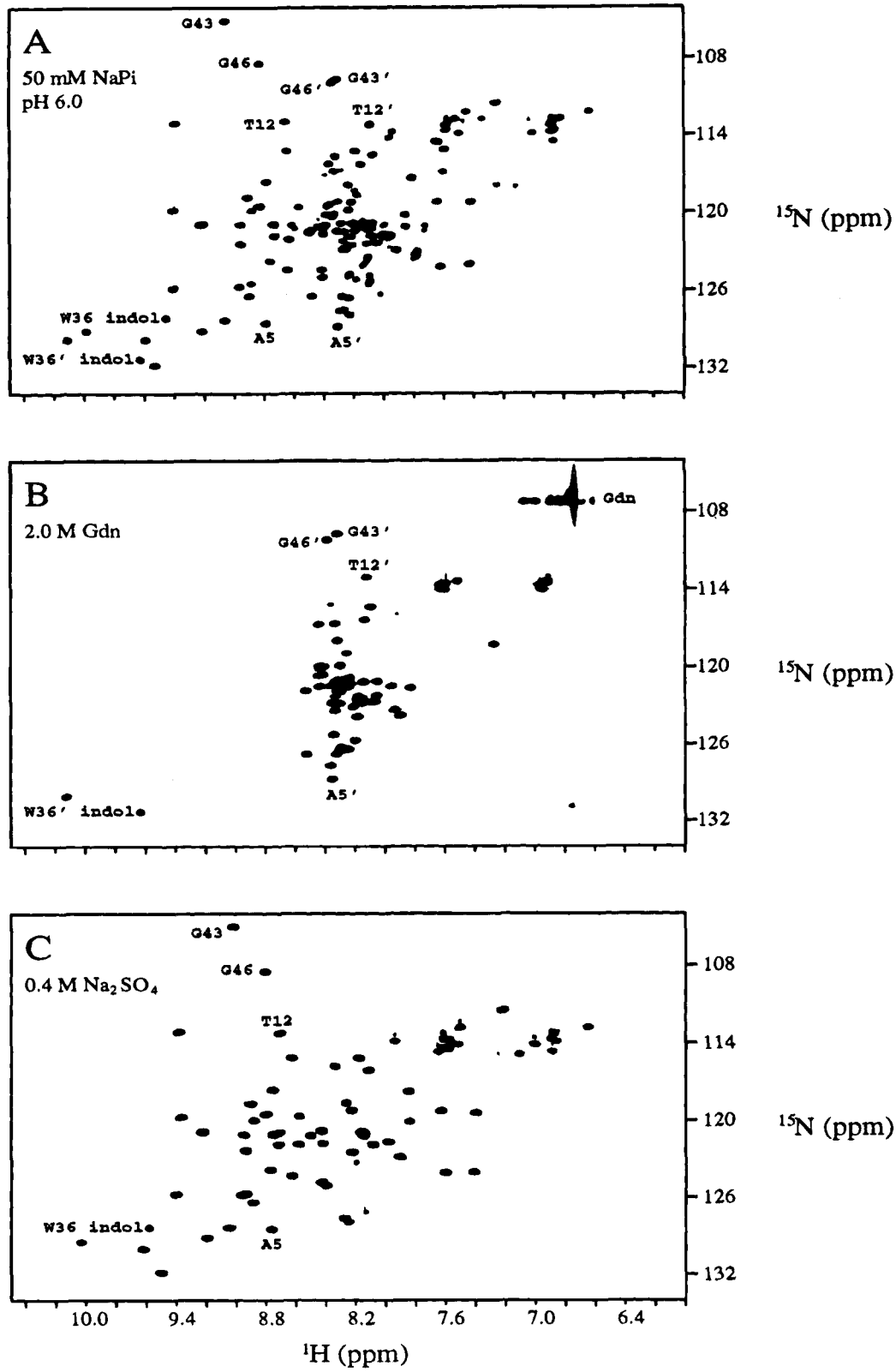


FIGURE 1: $^{15}N-^{1}H$ HSQC spectra of the drkN SH3 domain. (A) Equilibrium mixture of folded and unfolded states in 50 mM sodium phosphate, pH 6, 23 °C. Note the peaks of nearly equal intensity for the side chain Trp-36 indole group in folded (W36) and unfolded (W36′) states. Selected backbone amide resonances of folded (A5, T12, G43, G46) and unfolded (A5′, T12′, G43′, G46′) states have also been labeled with the one-letter amino acid code. (B) Completely denatured form in 2 M Gdn, 50 mM sodium phosphate, 23 °C. (C) Fully stabilized folded form in 0.4 M $Na_2SO_4$, 50 mM sodium phosphate, pH 6, 23 °C.

residues was found in the $^{15}N-^{1}H$ HSQC spectrum (Figure 1A) of a sample of 1 mM drkN SH3 domain in 50 mM sodium phosphate, pH 6.0, 23 °C. The possibility of slow conformational exchange on the NMR time scale between folded and unfolded forms of the drkN SH3 domain was confirmed by titrations with stabilizing and destabilizing agents (Figure 2; Table 1). Addition of Gdn caused the progressive disappearance of the resonances of the folded state and a simultaneous increase in intensity for the resonances of the unfolded state. The HSQC spectrum at 2 M Gdn (Figure 1B) showed the expected number of resonances for a 59-residue protein, with amide proton

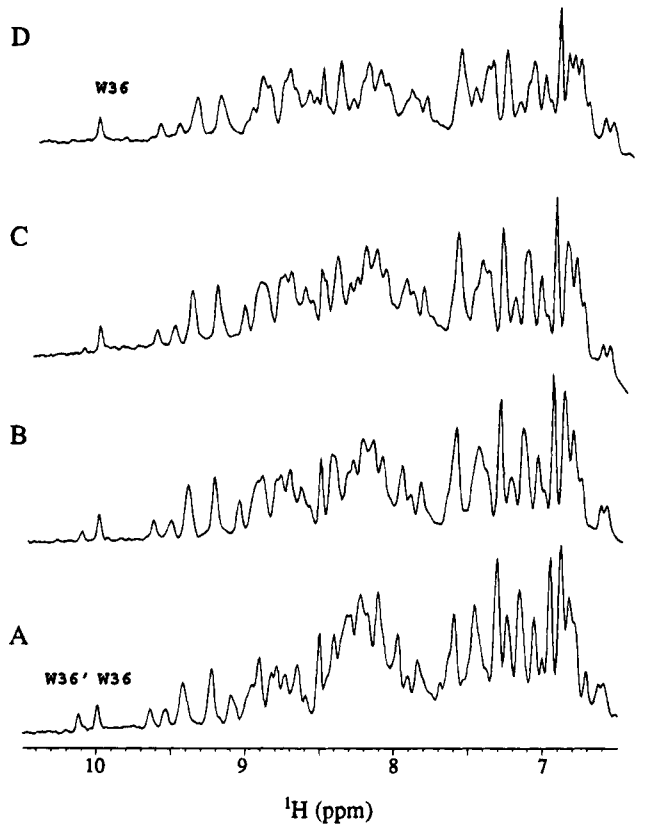


FIGURE 2: Downfield region of 1D NMR spectra from a $Na_2SO_4$ titration of the drkN SH3 domain in 50 mM sodium phosphate, pH 6, 23 °C. (A) 0 mM $Na_2SO_4$, (B) 125 mM $Na_2SO_4$, (C) 250 mM $Na_2SO_4$ and (D) 500 mM $Na_2SO_4$. Note the changes in the relative ratio of the two resonances of the side chain Trp-36 indole of folded (W36) and unfolded (W36′) states.

Table 1: Titration Data of the Shift in Equilibrium between Folded and Unfolded States of the drkN SH3 Domain[a]

| [Gdn] (M) | % folded[b] | pH | % folded | [$Na_2SO_4$] (mM) | % folded | temp (°C) | % folded |
|---|---|---|---|---|---|---|---|
| 0.0 | 45 | 3.0 | 28 | 0 | 65 | 23 | 70 |
| 0.3 | 20 | 6.0 | 65 | 125 | 70 | 30 | 60 |
| 0.6 | 10 | 7.5 | 62 | 250 | 85 | 45 | 25 |
| 1.0 | 0 | | | 500 | | 100 | |

[a] Values are based on intensities of the Trp-36 side chain indole resonance in 1D or 2D HSQC spectra. Percentage of folded was measured to within ±7% on samples of ~1 mM drkN SH3 domain in 50 mM sodium phosphate (pH 6) to which Gdn, $Na_2SO_4$, or small amounts of 0.1 N HCl and 0.1 N NaOH were added. All measurements were made at 30 °C except for the 23 and 45 °C temperature titration points. [b] The unusually low percentage of folded protein for the Gdn titration is due to the use of a slightly aggregated sample for this measurement.

chemical shifts clustered between 8 and 8.5 ppm, characteristic of an unfolded protein (Wüthrich, 1986). The addition of $Na_2SO_4$, in contrast, caused the progressive disappearance of the resonances of the unfolded state (Figure 2). Sulfate is at the extreme end of the Hofmeister series of inorganic anions and has been shown to stabilize protein structure due to solvent effects (Arakawa & Timasheff, 1985). An HSQC spectrum of a sample dissolved in 0.4 M $Na_2SO_4$ (Figure 1C) shows the expected number of resonances for a 59-residue protein, having the chemical shift dispersion characteristic of a folded protein (Wüthrich, 1986). Temperature and pH titrations demonstrate that the folded form is partially stabilized at low temperatures and neutral pH and the unfolded state is favored at high temperatures or low pH. The rate of exchange between folded and unfolded states in aqueous buffer conditions was estimated to be approximately 1 $s^{-1}$ using [$^{15}N$,$^1H$] exchange difference experiments (Wider et al., 1991). A method for the simultaneous determination of relaxation and exchange rates (Farrow et al., 1994) was also applied, yielding an average rate of exchange of 0.9 ± 0.2 $s^{-1}$ (Farrow et al., 1995).

NMR data from the two sets of exchanging resonances in the 3D spectra (Figure 3A,B) are consistent with the identification of the conformations as folded and unfolded. Chemical shifts of aliphatic resonances, particularly those of the $C^\alpha H$ protons, in this unfolded state are similar to literature values for random coil structure, while those of the folded form show large perturbations including downfield shifts characteristic of β-structure (Wishart et al., 1991). The average intensity of the amide−water exchange peaks from the $^{15}N$ TOCSY-HSQC for the folded form is much less than that of exchange peaks with amides of the unfolded state, demonstrating hydrogen bonding and less solvent exposure for amides in the folded protein structure. $^3J_{HN\alpha}$ coupling constants were also measured for nearly all of the residues in both folded and unfolded states at 25 °C (Forman-Kay et al., 1990), with higher values (~8 Hz) characteristic of β-structure seen for many residues in the folded state and lower values (~6 Hz) indicative of conformational averaging in the unfolded state (Karplus, 1963; Pardi et al., 1984). Overall, the pattern of NOEs, chemical shift differences from random coil, $^3J_{HN\alpha}$ couplings, and amide exchange rates for the unfolded state is quite different from those observed for the folded state, and the results suggest that the unfolded state, for the most part, is flexible and disordered.

The results from chemical shift differences from random coil, $^3J_{HN\alpha}$ couplings, amide−water exchange rates, and NOE patterns have been interpreted simply in terms of structure in either the folded or the unfolded states of the drkN SH3 domain. Under conditions of slow exchange, as we observe in this system, there should be little measured contribution to either the chemical shifts or the $^3J_{HN\alpha}$ couplings of the unfolded state from those of the folded state. It is very unlikely that there is a contribution to the NOE intensities for the unfolded state from the folded, since this would require magnetization to start on the unfolded state, interconvert with the folded state, NOE to a different proton of the folded state, and then interconvert back to the unfolded state during the mixing time. The presence of NOEs in the folded state which are absent in the unfolded state and vice versa is evidence that this second-order effect is insignificant, in addition to the overall lack of correlation of NOE intensities between the two states. Substantial errors due to contributions from interconverting states in the qualitative estimates of the amide−water exchange rates established on the basis of the intensities of the amide−water cross-peaks in the $^{15}N$ TOCSY-HSQC experiment are also unlikely. Contributions to the amide−water exchange peaks for the folded state from the unfolded state requires that the magnetization start on water and exchange with an NH in the unfolded state which subsequently interconverts to the folded state during the short (55 ms) TOCSY mixing period. This is a minor effect due to the slow (~1 $s^{-1}$) interconversion rate between the folded and unfolded states. Since certain residues have an intense amide−water exchange peak in the unfolded state and no exchange peak in the folded state (for example, Glu-45) while other residues have a weak or absent amide−water exchange peak in both the folded

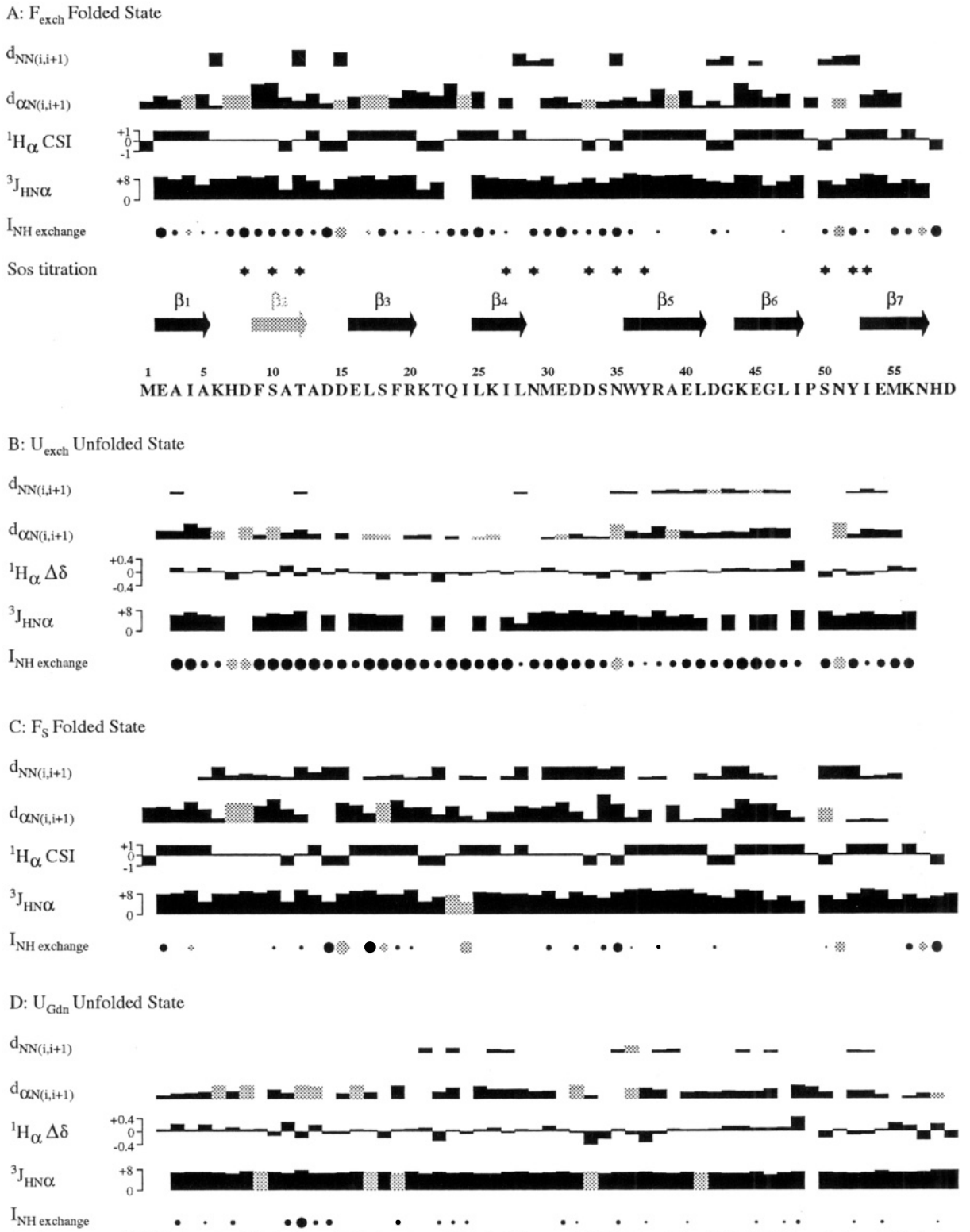


FIGURE 3: Summary of NMR data for (A) the $F_{exch}$ folded state and (B) the $U_{exch}$ unfolded state of the drkN SH3 domain in equilibrium in 50 mM sodium phosphate, pH 6, 30 °C, and for (C) the fully stabilized $F_S$ form in 0.4 M $Na_2SO_4$ and (D) the $U_{Gdn}$ denatured state in 2 M Gdn. Sequential $NH_i-NH_{i+1}$ [$d_{NN(i,i+1)}$) and $C^\alpha H_i-NH_{i+1}$ [$d_{\alpha N(i,i+1)}$) NOEs, differences in $C^\alpha H$ proton chemical shifts from random coil values, $^3J_{HN\alpha}$ coupling constants and intensity of amide−water exchange peaks are given. Residues whose amide $^1H$ or $^{15}N$ resonances broadened significantly or whose chemical shifts changed by more than 0.1 or 0.5 ppm, respectively, upon binding of a C-terminal fragment of Sos are denoted by a star in (A). The $\beta$-strands present in the $F_{exch}$ folded state are shown as black arrows above the sequence of the SH3 domain given below part (A) of the figure. The grey arrow shows the location of an irregular strand identified in the structure of the N-terminal SH3 domain of the homologous GRB2, and all strands are numbered as described for that structure (Wittekind et al., 1994). The thickness of the sequential connectivities denotes the relative NOE intensities observed in 150 ms mixing time 3D $^{15}N$-edited NOESY-HSQC spectra; grey lines reflect ambiguities in the measurement due to resonance overlap. The $C^\alpha H$ proton chemical shifts for the folded states are given in terms of the chemical shift index, $^1H^\alpha$ CSI, and for the unfolded states as differences from random coil values, $^1H^\alpha$ Δδ (Wishart et al., 1992). The intensities of the amide−water exchange peaks, $I_{NH\ exchange}$, are qualitative estimates of the strength of cross-peaks taken from 55 ms mixing time 3D $^{15}N$-edited TOCSY-HSQC spectra. Grey cirles reflect ambiguity in the estimates arising due to degeneracy of the water resonance with $C^\alpha H$ proton chemical shifts. NOE intensities and intensities of amide−water exchange peaks have been normalized to reflect the differences in populations of folded and unfolded states so that they can be directly compared. Data are missing for amides of Met-1 of all states, Asp-59 of the $F_{exch}$ folded state, Glu-2 of the unfolded states, and Asn-57 to Asp-59 of the $U_{exch}$ unfolded state due to unassigned resonances.

and unfolded states (such as Leu-28 and Tyr-37), their intensities are clearly not tightly correlated.

We recognize, however, that the estimates of the amide–water exchange rates based on the intensity of the amide–water cross-peak in the $^{15}N$ TOCSY-HSQC contain potential errors from a number of sources. These include (1) differences in loss of diagonal intensity due to variations in the TOCSY transfer efficiency for each residue, affected by the $^3J_{HN\alpha}$ couplings, (2) overlap with intraresidue NH–C$^\alpha$H TOCSY peaks, and (3) ROESY effects representing through-space amide–water interactions. Since the chemical shifts of the C$^\alpha$H resonances are known, interpretation of data from residues whose C$^\alpha$H shifts are at the water frequency can be made with caution. These residues are marked with grey circles in Figure 3. Because the rates determined are qualitative and have been utilized primarily for comparative purposes among the different states, the intensity estimates given in Figure 3 also have not been corrected for sequence dependences of the amide exchange rate. In order to better enable utilization of these estimates of amide-water exchange for relative comparisons, we have normalized the intensities of the water-amide exchange peaks from the different states taking into account the different populations in each state. NOE intensities have also been normalized in the same manner.

*Folded State (in Exchange with Unfolded State in Low Ionic Strength).* The secondary structure and overall topology of the folded state ($F_{exch}$) of the SH3 domain in exchange with the unfolded state in low ionic strength were derived from a qualitative analysis of the $^3J_{HN\alpha}$ coupling constants, sequential NOEs, amide–water exchange peak intensities from the $^{15}N$-edited TOCSY, and the C$^\alpha$H chemical shift index (Wishart et al., 1992). The results are consistent with those observed in previous structural studies of SH3 domains of other proteins. Figure 3A provides a summary of these data for the $F_{exch}$ folded state of the drkN SH3 domain. Six $\beta$-strands can be identified which correspond closely to those identified in the solution structure of the N-terminal SH3 domain of the mammalian homologue of drk, GRB2 (Wittekind et al., 1994). These strands include residues Glu-2 to Ala-5 ($\beta$1), Glu-16 to Arg-20 ($\beta$3), Leu-25 to Leu-28 ($\beta$4), Trp-36 to Leu-41 ($\beta$5), Lys-44 to Ile-48 ($\beta$6), and Ile-53 to Asn-57 ($\beta$7). Strands $\beta$4, $\beta$5, and $\beta$6 comprise a three-stranded antiparallel $\beta$-sheet, and strands $\beta$1 and $\beta$7 are involved in a second antiparallel sheet. A schematic diagram of the interstrand NOEs observed in the NOESY spectra of the exchanging system for the $F_{exch}$ folded state of the drkN SH3 domain and of the topology of the two primary $\beta$-sheets is shown in Figure 4. There are no obvious interstrand NOEs connecting $\beta$3 to either of the two sheets. The pattern of amide exchange and NOESY peaks, however, is consistent with the structure of the N-terminal GRB2 SH3 domain in which $\beta$3 has antiparallel hydrogen bonds with an irregular extended stretch of residues following $\beta$1, termed $\beta$2. Note in particular the weak or absent amide exchange peaks for residues of $\beta$5 and $\beta$6, demonstrating the stability of the $\beta$-structure for these two strands.

Chemical shift changes and resonance broadening for specific residues of the SH3 binding site were observed upon addition of a portion of the C-terminal tail of Sos, a biological target of the drkN SH3 domain (Olivier et al., 1993), demonstrating that the $F_{exch}$ folded state retains its binding activity. The Sos fragment comprised residues 1314–1386, encompassing two polyproline PPPxPPR sequences. The

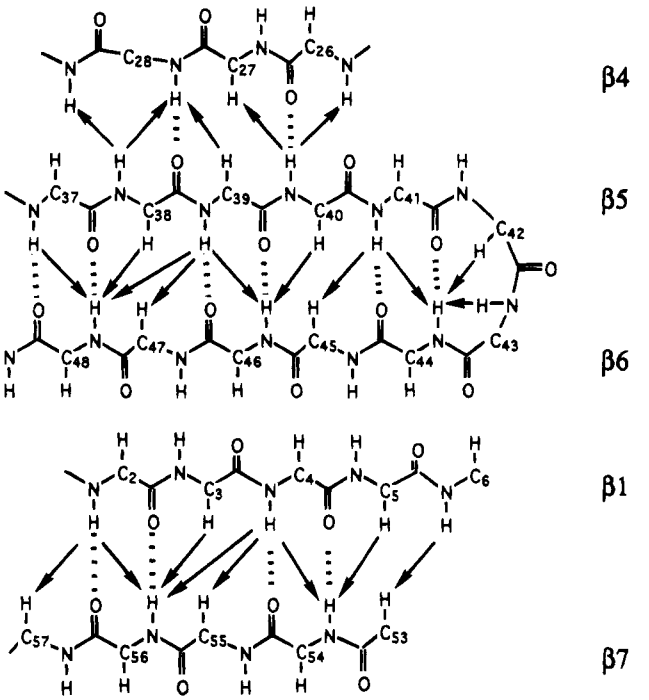


FIGURE 4: Schematic diagram of the topology of the two antiparallel $\beta$-sheets for which cross-strand NOEs were observed in the $F_{exch}$ folded state of the drkN SH3 domain in equilibrium with the unfolded state in low ionic strength. Cross-strand NOEs are denoted with arrows, and hydrogen bonds defined by these NOEs and amide protons which weakly exchange with solvent are marked with a dashed line.

residues of the drkN SH3 domain which showed spectral changes, indicated in Figure 3A, correspond to homologous resonances of Src, p85, and the C-terminal GRB2 SH3 domains which were perturbed upon binding proline-rich peptides (Yu et al., 1992; Booker et al., 1993; Kohda et al., 1994). Additionally, these positions map to residues in structures of SH3 domain–peptide complexes showing SH3 domain–peptide interactions (Musacchio et al., 1994; Yu et al., 1994; Feng et al., 1994; Wittekind et al., 1994; Teresawa et al., 1994; Goudreau et al., 1994).

*Fully Stabilized Folded State (in 0.4 M $Na_2SO_4$).* All NOEs observed for the $F_{exch}$ folded state are a subset of those observed in the fully stabilized ($F_S$) folded state in 0.4 M $Na_2SO_4$. An estimate of the number of NOEs which were observed for the $F_{exch}$ folded state as a percentage of NOEs observed in the $F_S$ folded state can be made based on comparison of the $^{15}N$-edited NOESY spectra of the exchanging sample and of the $F_S$ folded state. (Aliphatic–aliphatic NOEs were not measured for the $F_{exch}$ folded state because of spectral ambiguities arising from the degeneracy of aliphatic chemical shifts in the unfolded state and lack of assignments for these resonances.) The $^{15}N$-edited NOESY for the exchanging sample contains 268 NOEs involving only resonances of the $F_{exch}$ folded state, many of which are intraresidue or sequential NOEs. This is 43% of the 618 NOEs observed in the $^{15}N$-edited NOESY spectrum of the $F_S$ folded state. Since chemical exchange between the folded and unfolded states decreases the intensities of NOE cross-peaks between $^1$Hs of the $F_{exch}$ folded state and since the population of folded molecules comprises only about 60% of the total molecules in the exchanging sample, it is not surprising that the NOE intensities for the $F_{exch}$ folded state are weaker and fewer peaks are observed than for the $F_S$

folded state. The structures of these two folded states, in low and high ionic strength, appear to be the same since backbone $C^{\alpha}H$ and $^{15}N$ chemical shifts [Figure 6A−C (left side; top, middle, and bottom panels, respectively)] and $^{3}J_{NH\alpha}$ coupling constants (Figure 3A,C) are nearly identical. The $C^{\beta}H$ chemical shifts are also essentially identical, and the sequential NOE patterns are very similar (Figure 3A,C). The $C^{\alpha}H$ shifts, especially, are exquisitely sensitive to conformation, while the NH chemical shifts are more sensitive to differences in solvent conditions than the $C^{\alpha}H$ or $^{15}N$ shifts, indicating that caution must be used in the interpretation of differences between the states for these NH shifts. Thus, while the possibility cannot be ruled out that the salt stabilizes a slightly different structure in the $F_S$ folded state from the $F_{exch}$ folded state where a smaller number of NOEs are observed, due to the correspondence of chemical shifts, couplings constants, and NOE patterns any differences must be extremely small. Structural parameters for both of these folded states are in close agreement with the recently determined solution structure of the homologous N-terminal SH3 domain of GRB2 (Wittekind et al., 1994).

Protection from amide exchange with water in the $F_S$ folded state, however, is significantly greater than in the $F_{exch}$ folded state. The effect of high salt on solvent structure may play a role, but the increase in the overall stability of the domain is clearly a primary factor. The addition of 0.4 M $Na_2SO_4$ to the sample increases the ratio of folded to unfolded states from 60:40 to greater than 99:1. This corresponds to an increase in the stability as measured by the $\Delta G_{folding}$ from 0.2 kcal/mol to at least 2.8 kcal/mol.

*Unfolded State (in Exchange with Folded State in Low Ionic Strength).* Figure 3B illustrates the evidence for structure in the unfolded state ($U_{exch}$) of the drkN SH3 domain in 50 mM sodium phosphate, pH 6 and 30 °C, including sequential NOE patterns, the difference between the random coil chemical shifts for the $C^{\alpha}H$ proton and the observed shifts, the measured $^{3}J_{HN\alpha}$ coupling constants, and the degree of amide−water exchange. The chemical shifts of most of the $C^{\alpha}H$ protons are close to the expected random coil values (Wishart & Sykes, 1994). The chemical shift for the $C^{\alpha}H$ of Ile-48 which deviates significantly downfield from the cited random coil value is most likely due to its location immediately N-terminal to a proline (Wishart et al., 1995). The $^{3}J_{HN\alpha}$ couplings are all between 5 and 8 Hz, with many between 6 and 7 Hz, expected if the backbone torsion angles average over allowed regions of conformational space. An exception to this is found for residue Leu-28 which has a coupling of less than 4 Hz and a sequential $NH_i-NH_{i+1}$ NOE, consistent with a turn structure. (These values contrast with the folded states for which half of the measured $^{3}J_{HN\alpha}$ couplings are greater than 8 Hz and the Leu-28 coupling is 7.9−8.0 Hz.) The weak amide−water exchange peaks for Leu-28, Trp-36, Tyr-37, Arg-38, and Ile-53 are supportive of the protection of these positions by the presence of transiently stable structure in certain regions of the unfolded state. Although the sequence dependence of the amide exchange rate for bulky residues, such as leucines and isoleucines, contributes to this protection from exchange (Bai et al., 1993), comparison with other leucines, arginines, and isoleucines in the protein which show significant amide−water exchange (Ile-4, Leu-17, Arg-20, Ile-24, Leu-25, and Ile-27) confirms that the sequence dependence is not the major factor.

Sequential $C^{\alpha}H_i-NH_{i+1}$ NOEs are observed over a significant portion of the domain, corresponding to allowed interproton distances of between 2.2 and 3.6 Å for all $C^{\alpha}H_i-NH_{i+1}$ pairs. However, there are a number of residues for which these NOEs are absent, including residues Ile-27 to Met-30. Sequential $NH_i-NH_{i+1}$ NOEs, diagnostic of residual helical or turn-like structure in folded proteins, are seen for residues Ala-3 to Ile-4, Thr-12 to Ala-13, Leu-28 to Asn-29, Asn-35 to Tyr-37, Arg-38 to Ile-48, and Tyr-52 to Met-55. In addition to the steep dependence on distance, the intensity of an NOE in the macromolecular limit is also proportional to the spectral density function evaluated at zero frequency, $J(0)$, which is sensitive to dynamic processes. $J(0)$ values for 12 backbone positions including 4 in the region from Asn-35 to Ile-48 were determined by Farrow et al. (1995) with NMR pulse sequences developed to probe the $^{15}N$ relaxation rates of the two exchanging species (Farrow et al., 1994) and were used to analyze the relative contributions of structural preferences and dynamic behavior to the observed NOE intensities. Neither the intensity of sequential $C^{\alpha}H_i-NH_{i+1}$ NOEs nor the presence or intensity of sequential $NH_i-NH_{i+1}$ NOEs correlates with the $J(0)$ values; therefore, these sequential $NH_i-NH_{i+1}$ NOEs must reflect some structural preference for the α region of $\varphi-\psi$ space for residues 35−48 and not merely differences in dynamic behavior from the rest of the protein.

The C-terminal region of the $U_{exch}$ unfolded state of the drkN SH3 domain from Asn-35 to Met-55 may therefore be described as an ensemble of rapidly conformationally averaging structures which preferentially sample the α-region of $\varphi-\psi$ space. The $U_{exch}$ unfolded state of the drkN SH3 domain, however, does not contain stable helical structure. The presence of both $NH_i-NH_{i+1}$ and some stronger $C^{\alpha}H_i-NH_{i+1}$ NOEs in this region must be interpreted as conformational exchange between turn-like and extended states with minimal cooperativity toward formation of longer helical stretches. This "structure" of the C-terminal region including residues Asn-35 to Ile-48 is not native-like, as it corresponds to two of the most stable $\beta$-strands in the $F_{exch}$ folded state of the SH3 domain, $\beta5$ and $\beta6$. The absence of a continuous stretch of sequential amide−amide NOEs for residues of strands $\beta5$, $\beta6$, and $\beta7$ in the folded state (Figure 5A) demonstrates the difference in the structures of these two states. On the basis of the intensity of sequential $NH_i-NH_{i+1}$ NOEs from Asn-35 to Ile-48 in the unfolded state (Figure 3B, Figure 5B), it appears that the residues in this region in a significant fraction of the molecules in the $U_{exch}$ unfolded state appear to adopt turn-like conformations in rapid exchange with more extended conformations. Weak amide−water exchange peaks are also seen for a number of residues in this region, as noted previously, particularly from Trp-36 to Ala-39, further evidence of the presence of transient hydrogen bonding or hydrophobic burial.

It is interesting to note that the data from NOEs, chemical shifts, coupling constants, and water−amide hydrogen exchange peaks for the $U_{exch}$ unfolded state are also not highly correlated. This may be explained by the different ways that these experimental parameters are averaged over an exchanging ensemble of structures. Due to the nature of the dependence of the NMR observables on structural properties of the molecule, the average value measured over a rapidly exchanging ensemble such as a predominantly unfolded protein will be a simple population weighted average in the case of the chemical shift. An NOE intensity

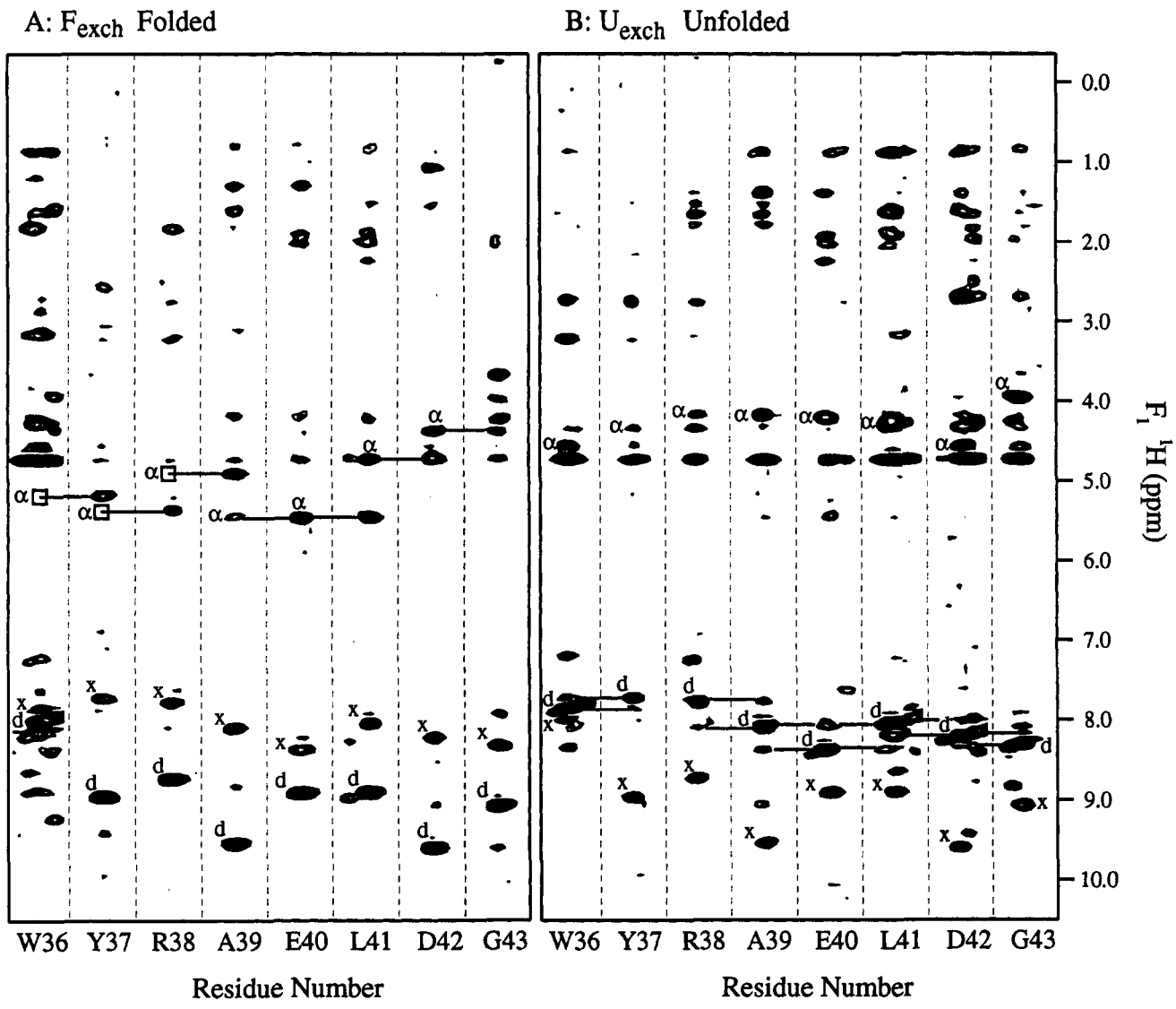


FIGURE 5: Amide strips from a 150 ms 3D $^{15}N$-edited NOESY-HSQC experiment for residues Trp-36 to Gly-43, for the $F_{exch}$ folded (A) and $U_{exch}$ unfolded (B) states of the drkN SH3 domain in 50 mM sodium phosphate, pH 6, 30 °C. Data were recorded simultaneously for the two states in this exchanging system. The sequential $C^{\alpha}H_i-NH_{i+1}$ peaks are indicated for the folded state, and $NH_i-NH_{i+1}$ peaks are indicated for the unfolded state. Intraresidue $C^{\alpha}H_i-NH_i$ peaks are labeled α; the chemical shift of the $C^{\alpha}H$ is marked by a box where the peak is absent. Exchange peaks (labeled x) between the amide diagonal peaks (labeled d) of the folded and unfolded states can be clearly seen. Water−amide exchange peaks are observed at the water chemical shift of 4.7 ppm ($F_1$). Note that these intensities are greater than those observed in the 55 ms 3D $^{15}N$-edited TOCSY-HSQC due to the longer mixing time.

averages as $\langle r^{-6} \rangle$ or $\langle r^{-3} \rangle^2$ (Kessler, 1988), depending on whether the averaging is rapid compared to the rate of molecular tumbling, where $r$ is the distance between the two involved protons. A $J$ coupling averages as a cosine modulated function of the $\varphi$ torsion angle. The water−amide exchange rate, while predominantly a population weighted average, is often difficult to interpret, especially since stable amide protection is not always temporally associated with the formation of structure in proteins. Thus, residual structure which is present for only a fraction of the time, perhaps in relatively small amounts, may only be observed with a particularly sensitive parameter, such as the NOE, but not confirmed by other structural data.

*Denatured State (in 2 M Gdn).* In order to compare the $U_{exch}$ unfolded state present in aqueous buffer at low ionic strength with an unfolded state under denaturing conditions, we assigned and analyzed NMR data from the backbone resonances of the drkN SH3 domain denatured in 2 M Gdn ($U_{Gdn}$ state). Figure 3D shows the sequential NOEs, differences from the $C^{\alpha}H$ random coil chemical shifts, $^3J_{HN\alpha}$ coupling constants, and degree of amide proton exchange with solvent for the $U_{Gdn}$ unfolded state. The most striking differences between the two unfolded states are the loss of the extremely low $^3J_{HN\alpha}$ coupling at residue Leu-28 and the overall reduction of amide proton exchange with solvent in 2 M Gdn. The loss of residual structure may be rationalized in the highly denaturing solution conditions employed. Potential hydrogen bonding of the Gdn with backbone carbonyls may shield backbone amide protons from exchange with water. The extended stretch of sequential $NH_i-NH_{i+1}$ NOEs is also disrupted.

Comparison of the backbone $C^{\alpha}H$, NH, and $^{15}N$ chemical shifts of the two unfolded states, shown in Figure 6D−F, demonstrates that there are significant differences centered around residues Arg-20 to Gln-23 and extending over a range of 15−20 residues. Other local differences are also observed throughout the domain, particularly at His-7 and Asp-8, providing further evidence for structural differences in the unfolded states. His-7 and Asp-8, located in the loop between β1 and β2, and Arg-20 to Gln-23, in the loop

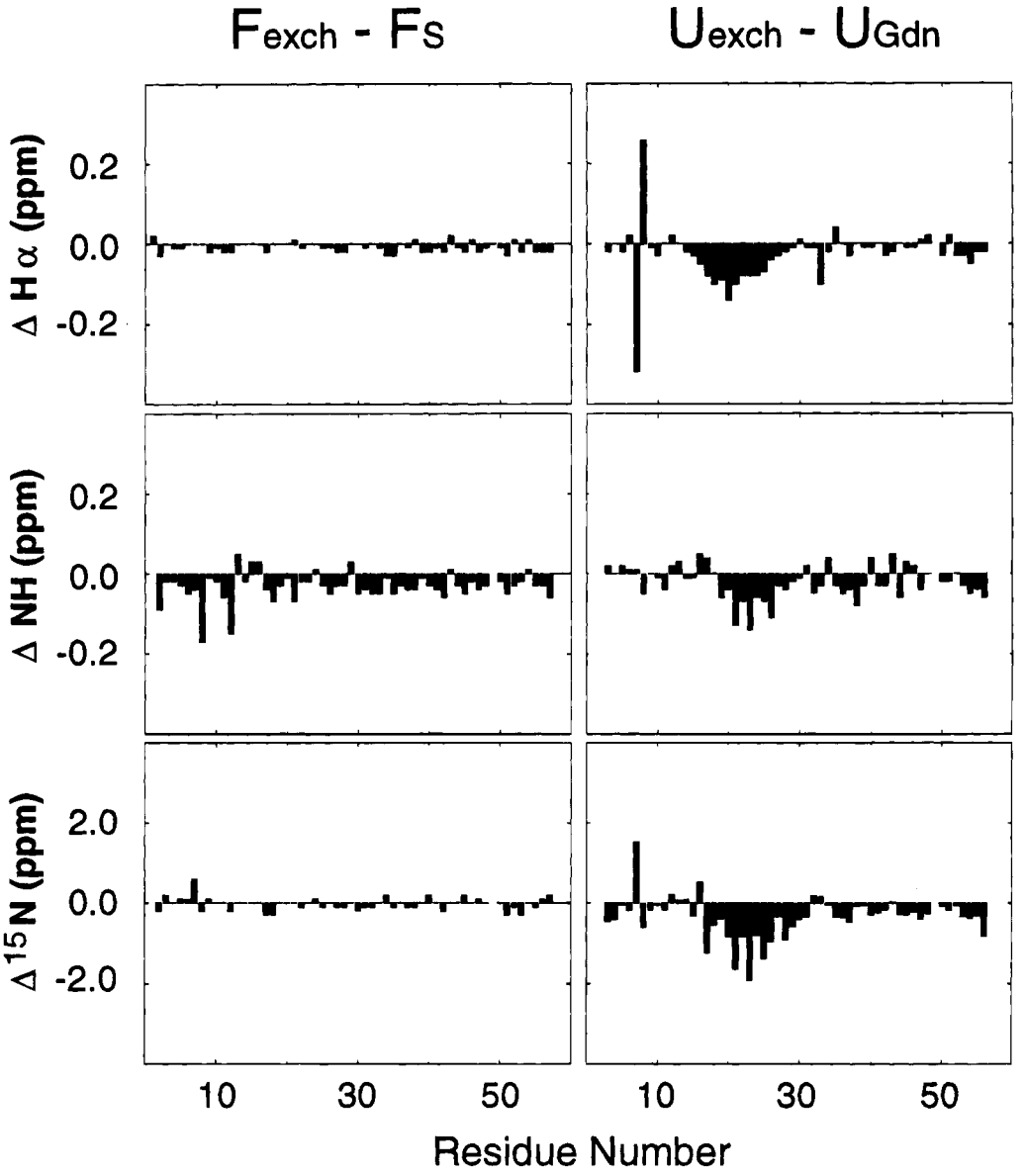


FIGURE 6: Differences in backbone $C^{\alpha}H$, NH, and $^{15}N$ chemical shifts of the two folded and the two unfolded states of the drkN SH3 domain. Differences between the chemical shifts of the $F_{exch}$ folded state in low ionic strength buffer and the $F_S$ folded state in 0.4 M $Na_2SO_4$ are shown in panels A–C (left side: top, middle, and bottom panels, respectively) and between the $U_{exch}$ unfolded state in low ionic strength buffer and the $U_{Gdn}$ denatured state in 2 M Gdn in panels D–F (right side; top, middle, and bottom panels, respectively).

between $\beta$3 and $\beta$4, are in close contact in the folded structure. The fact that correlated chemical shift changes are observed between the $U_{exch}$ unfolded state and the $U_{Gdn}$ denatured state at these positions is suggestive of residual interactions between the $\beta$1–$\beta$2 loop and $\beta$3–$\beta$4 loop regions in the $U_{exch}$ unfolded state which are disrupted in Gdn. As Shortle has noted in a recent review (Shortle, 1993), unfolded states are extremely sensitive to the conditions of denaturation. Studies of urea- and Gdn-denatured FKBP also revealed differences in the structure of the states (Logan et al., 1994). Therefore, our investigation of the nature of the unfolded state of the drkN SH3 domain under identical conditions to those in which the folded state is present is likely to shed insight into states of proteins during *in vivo* synthesis and folding.

*Implications for the Folding Pathway.* The finding of preferences for turn-like conformations in the $U_{exch}$ unfolded state in regions of stable $\beta$-structure in the folded form raises the question of whether these transient turns can be viewed as intermediates on the folding pathway for the predominantly $\beta$-structured SH3 domain. That this state interconverts with the $F_{exch}$ folded state approximately once per second argues against viewing it as the terminal point of a dead-end folding pathway. The chemical shift changes and resonance broadening for specific residues observed upon addition of the C-terminal tail of Sos demonstrate that the $F_{exch}$ folded state in this exchanging system retains its binding activity. The activity of the $F_{exch}$ folded state and its structure which is consistent with other known SH3 structures support the biological relevance of the structural results for the $U_{exch}$ unfolded state which exists in equilibrium with the folded state in 50 mM sodium phosphate, pH 6. In addition, the backbone chemical shifts, $^3J_{HN\alpha}$ coupling constants, and sequential NOE patterns of the $F_S$ folded state in 0.4 M $Na_2SO_4$ are virtually indistinguishable from those of the $F_{exch}$ folded state in low ionic strength (Zhang et al., 1994), confirming the identity of the state as folded. Since many partially structured equilibrium "intermediates" are studied under denaturing conditions, the significance of any residual structure in this $U_{exch}$ unfolded state in 50 mM sodium phosphate, pH 6.0, 30 °C, cannot be dismissed.

It has been observed previously, using pulsed hydrogen exchange labeling, that stable helical structure forms within milliseconds during protein folding (Roder et al., 1988), yet stable $\beta$-structure in all-$\beta$ proteins forms only within 1−25 s (Varley et al., 1993). While $\beta$-sheets can form within milliseconds in mixed $\alpha-\beta$ proteins, the first sites of stable $\beta$-structure are localized to interactions with helical regions of the molecule (Varley et al., 1993; Bycroft et al., 1990; Briggs & Roder, 1992; Lu & Dalquist, 1992; Radford et al., 1992). We might speculate, then, that the formation of preferential turn-like structure in residues Asn-35 to Ile-48 nucleates the $\beta$-sheet containing strands $\beta$5 and $\beta$6. These transient turns could nucleate the $\beta$-hairpin turn from Leu-41 to Lys-44, allowing long-range interactions between residues of $\beta$5 and $\beta$6, catalyzing the formation of the $\beta$-sheet hydrogen bonding interactions. In addition to this region, the significant finding of a small $^3J_{HN\alpha}$ coupling and a sequential amide−amide NOE at residue Leu-28 demonstrates the presence of a stable turn which is not conformationally averaged. The absence of a low coupling in the folded state at Leu-28 reinforces the concept suggested above regarding non-native turns which nucleate $\beta$-structure. In the folded state, this residue is located at the C-terminus of strand $\beta$4 which hydrogen bonds to the C-terminal residues of $\beta$5. A homology model of the drkN SH3 domain was generated based on the recently published structure of the N-terminal SH3 domain of GRB2 (Wittekind et al., 1994), using the program QUANTA (Molecular Simulations Incorporated, University of York, York, England). Examination of the structure of residue Leu-28 in this model shows a turn having $\varphi$, $\psi$ angles of −85°, −29°, heading into an irregular extended region which interacts with the N-terminal residues of strand $\beta$5. This turn region in the unfolded state could be important for determining the ultimate alignment of strands $\beta$4 and $\beta$5.

Non-native helical structure, as evidenced by stretches of $NH_i-NH_{i+1}$ and $C^\alpha H_i-C_\beta H_i+3$ NOEs, was observed recently in the alcohol (50% trifluoroethanol) induced molten globule-like state of monellin (Fan et al., 1993) and in the urea- and Gdn-denatured states of FKBP (Logan et al., 1994). Assuming that partially structured states of proteins are models for protein folding intermediates, non-native structure could be significant in the mechanism of folding for certain proteins. The finding of non-native structure in the $U_{exch}$ unfolded state of the drkN SH3 domain supports this view. Since the presence and extent of structure for partially structured equilibrium "intermediates" can be dependent on the type of denaturation−urea, Gdn, alcohols, pH, or extremes of temperature (Shortle, 1993), the fact that this state exists in the absence of denaturant argues that the structure observed is likely to be relevant to the pathway under physiological folding conditions. The turn structure observed in this unfolded state can perhaps be seen as a model for the earliest folding intermediates based on the dynamic equilibrium of the unfolded state with the folded state and its presence in aqueous buffer conditions.

While the instability of the isolated drkN SH3 domain may be explained by loss of interactions with the remainder of the protein, it is possible that this equilibrium between folded and unfolded states exists in the intact drk, as well. Since drk has been found to be constitutively associated with Sos *in vivo* (Schlessinger, 1993), the absence of this target binding interaction could be primarily responsible for the instability of the isolated domain. Solution structures of Sos peptide complexes of the N-terminal SH3 domain of the homologous GRB2 have demonstrated the importance of a charge interaction involving an arginine in the proline-rich target peptides (Wittekind et al., 1994; Teresawa et al., 1994; Goudreau et al., 1994). This interaction is responsible for determining the directionality of the proline helix axis (Feng et al., 1994) and may be involved in stabilizing the structure of the SH3 domain in the complex with Sos. In the homology model of the drkN SH3 domain, there are seven negatively charged residues which are in close proximity to each other and lie near the peptide binding surface: Asp-14, Asp-15, Glu-16, Glu-31, Asp-32, Asp-33, and Glu-45. The arginines of Sos-derived peptides interact with this negatively charged cluster, specifically Glu-16. In the absence of Sos peptides, this interaction is removed which could lead to destabilization of the domain by electrostatic repulsion of the negative charge on the binding surface. Negative electrostatic repulsion on the surface of the SH3 domain has also been implicated in the reduced stability of the C-terminal SH3 domain of Sem-5 in low-salt buffers compared with that in 0.5 M NaCl (Lim et al., 1994). These authors suggest that target binding function may be enhanced by the excess of surface negative charge at the expense of the stability of the SH3 domain. The instability, especially in the case of the N-terminal SH3 domain of drk, may lead to increased proteolysis of the molecule and therefore could play a regulatory role by removing the protein from the cell when its target is unavailable for binding. This mode of regulation has also been suggested for other proteins (Pace, 1990; Arfin & Bradshaw, 1988).

It is interesting to note that other SH3 domains also demonstrate marginal stability. The N-terminal SH3 domain of GRB2, as mentioned previously, has been reported to exist in equilibrium between folded and unfolded states at pH 3.5 in water and to be unstable at pH 6 in 20 mM sodium phosphate and 100 mM NaCl (Goudreau et al., 1994). NMR studies of the Src (Yu et al., 1993), the N-terminal GRB2 (Goudreau et al., 1994), and the C-terminal GRB2 (Kohda et al., 1994) SH3 domains reported extremely few or no amide protons which exchange slowly with water, indicative of instability of the domain (*i.e.*, local or global unfolding which enables more rapid amide exchange in the extended state). While significant stability to thermal denaturation was seen for the C-terminal Sem-5 SH3 domain (Lim et al., 1994), the $\Delta G_{folding}$ of the spectrin SH3 domain (Viguera et al., 1994) was determined to be less than expected for a single domain protein. Further evidence of the instability of SH3 domains has been seen in the sensitivity of the isolated domains to precipitation. Since unfolded protein has significant amounts of exposed hydrophobic surface which can interact irreversibly at sufficiently high concentrations such as those normally utilized in NMR samples, precipitation can be a sign of protein instability, especially if it occurs over time. The C-terminal SH3 domain of GRB2 was found to precipitate at pH <7.5 (Kohda et al., 1994), and the C-terminal SH3 domain of drk was observed to precipitate over the course of a day at 23 °C in our laboratory (Y. Aubin, personal communication).

Studies of intact drk and multidomain fragments of drk are being pursued in order to address the stability of this domain in the entire molecule. Since it is the most N-terminal domain, studies of the folding pathway of the drkN SH3 domain should be relevant to an understanding of the folding of the intact drk, regardless of the stability of

the domain. The results of this investigation of the drkN SH3 domain point to a need for more studies of unfolded states of proteins under nondenaturing conditions in order to better understand their general nature and their physiological relevance.

## ACKNOWLEDGMENT

We thank Dr. Lewis Kay for many useful discussions and for guidance with the NMR spectroscopy. In addition, we thank Dr. Tony Pawson for his enthusiastic support of the project and Dr. Mike Wittekind for providing us with coordinates of the N-terminal SH3 domain of GRB2 prior to publication. We also acknowledge J. Paul Olivier for assistance in subcloning the drkN SH3 domain, Randall Willis for help with purification of the SH3 domain, and Dr. Mike Rosen for his involvement with the Sos titration experiment.

## REFERENCES

Arakawa, T., & Timasheff, S. N. (1985) *Methods Enzymol. 114*, 49.
Arfin, S. M., & Bradshaw, R. A. (1988) *Biochemistry 27*, 7979.
Bai, Y., Milne, J. S., & Englander, S. W. (1993) *Proteins: Struct., Funct., Genet. 17*, 75.
Bar-Sagi, D., Rotin, D., Batzer, A., Mandiyan, V., & Schlessinger, J. (1993) *Cell 74*, 83.
Booker, G. W., Gout, I., Downing, A. K., Driscoll, P. C., Boyd, J., Waterfield, M. D., & Campbell, I. D. (1993) *Cell 73*, 813.
Borchert, T. V., Mathieu, M., Zeelen, J. Ph., Courtneidge, S. A., & Wierenga, R. K. (1994) *FEBS Lett. 341*, 79.
Briggs, M. S., & Roder, H. (1992) *Proc. Natl. Acad. Sci.* U.S.A. *89*, 2017.
Bycroft, M., Matouschek, A., Kellis, J. T., & Fersht, A. R. (1990) *Nature 346*, 488.
Cicchetti, P., Mayer, B. J., Thiel, G., & Baltimore, D. (1992) *Science 257*, 803.
Creighton, T. E. (1992) *Science 256*, 111.
Delaglio, F. (1993) NMRPipe System of Software, National Institutes of Health, Bethesda, MD.
Englander, S. W., & Kallenbach, N. R. (1984) *Q. Rev. Biophys. 16*, 521.
Fan, P., Bracken, C., & Baum, J. (1993) *Biochemistry 32*, 1573.
Farrow, N. A., Zhang, O., Forman-Kay, J. D., & Kay, L. E. (1994) *J. Biomol. NMR 4*, 727.
Farrow, N. A., Zhang, O., Forman-Kay, J. D., & Kay, L. E. (1995) *Biochemistry 34*, 868.
Feng, S., Chen, J. K., Yu, H., Simon, J. A., & Schrieber, S. L. (1994) *Science 266*, 1241.
Flanagan, J. M., Kataoka, M., Shortle, D., & Engelman, D. M. (1992) *Proc. Natl. Acad. Sci. U.S.A. 89*, 748.
Forman-Kay, J. D., Gronenborn, A. M., Kay, L. E.,Wingfield, P. T., & Clore, G. M. (1990) *Biochemistry 29*, 1566.
Garrett, D. S., Powers, R., Gronenborn, A. M., & Clore, G. M. (1991) *J. Magn. Reson. 95*, 214.
Goudreau, N., Cornill, F., Duchesne, M., Parker, F., Tocqué, B., Garbay, C., & Roques, B. P. (1994) *Nat. Struct. Biol. 1*, 898.
Karplus, M. (1963) *J. Am. Chem. Soc. 85*, 2870.
Kay, L. E., & Bax, A. (1990) *J. Magn. Reson. 86*, 110.
Kay, L. E., Keifer, P., & Saarinen, T. (1992) *J. Am. Chem. Soc. 114*, 10663.
Kessler, H., Griesinger, C., Lautz, J., Muller, A., van Gunsteren, W. F., & Berendsen, H. J. C. (1988) *J. Am. Chem. Soc. 110*, 3393.
Koch, C. A., Anderson, D., Moran, M. F., Ellis, C., & Pawson, T. (1991) *Science 252*, 668.
Kohda, D., Hatanaka, H., Odaka, M., Madiyan, V., Ullrich, A., Schlessinger, J., & Inagaki, F. (1993) *Cell 72*, 953.
Kohda, D., Terasawa, H., Ichikawa, S., Ogura, K., Hatanaka, H., Mandiyan, V., Ullrich, A., Schlessinger, J., & Inagaki, F. (1994) *Structure 2*, 1129.
Koyama, S., Yu, H., Dalgarno, D. C., Shin, T. B., Zydowsky, L. D., & Schreiber, S. L. (1993) *Cell 72*, 945.
Kuriyan, J., & Cowburn, D. (1993) *Curr. Opin. Struct. Biol. 3*, 828.
Kuwajima, K., Sakuraoka, A., Fueki, S., Yoneyama, M., & Sugai, S. (1988) *Biochemistry 27*, 7419.
Lim, W. A., Farruggio, D. C., & Sauer, R. T. (1992) *Biochemistry 31*, 4324.
Lim, W., Fox, R. O., & Richards, F. M. (1994) *Protein Sci. 3*, 1261.
Logan, T. M., Thériault, Y., & Fesik, S. W. (1994) *J. Mol. Biol. 236*, 637.
Lu, J., & Dalquist, F. W. (1992) *Biochemistry 31*, 4749.
Musacchio, A., Gibson, T., Lehto, V.-P., & Saraste, M. (1992a) *FEBS Lett. 307*, 55.
Musacchio, A., Noble, M., Paupit, R., Wierenga, R., & Saraste, M. (1992b) *Nature 359*, 851.
Musacchio, A., Saraste, M., & Wilmanns, M. (1994) *Nat. Struct. Biol. 1*, 546.
Neri, D., Billeter, M., Wider, G., & Wüthrich, K. (1992) *Science 257*, 1559.
Noble, M. E. M., Musacchio, A., Saraste, M., Courtneidge, S. A., & Wierenga, R. K. (1993) *EMBO J. 12*, 2617.
Olivier, J. P., Raabe, T., Henkemeyer, M., Dickerson, B., Mbamalu, G., Margolis, B., Schlessinger, J., Hafen, E., & Pawson, T. (1993) *Cell 73*, 179.
Pace, C. N. (1975) *CRC Crit. Rev. Biochem. 3*, 1.
Pace, C. N. (1990) *Trends Biochem. Sci. (Pers. Ed.) 15*, 14.
Pardi, A., Billeter, M., & Wüthrich, K. (1984) *J. Mol. Biol. 180*, 741.
Pawson, T., & Gish, G. D. (1992) *Cell 71*, 359.
Ptitsyn, O. B., Pain, R. H., Semisotnov, G. V., Zerovnik, E., & Razgulyaev, O. I. (1990) *FEBS Lett. 262*, 20.
Radford, S. E., Dobson, C. M., & Evans, P. A. (1992) *Nature 358*, 302.
Rashin, A. A. (1987) *J. Mol. Biol. 198*, 339.
Roder, H., Elöve, G. A., & Englander, S. W. (1988) *Nature 335*, 700.
Schlessinger, J. (1993) *Trends Biochem. Sci. (Pers. Ed.) 18*, 273.
Shortle, D. (1993) *Curr. Opin. Struct. Biol. 3*, 66.
Simon, M. A., Dodson, G. S., & Rubin, G. M. (1993) *Cell 73*, 169.
Teresawa, H., Kohda, D., Hatanaka, H., Tsuchiya, S., Ogura, K., Nagata, K., Ishii, S., Mandiyan, V., Ullrich, A., Schlessinger, J., & Inagaki, F. (1994) *Nat. Struct. Biol. 1*, 891.
Udgaonkar, J. B., & Baldwin, R. L (1988) *Nature 335*, 694.
Varley, P., Gronenborn, A. M., Christense, H., Wingfield, P. T., Pain, R. H., & Clore, G. M. (1993) *Science 260*, 1110.
Viguera, A. R., Martinez, J. C., Filimonov, V. V., Mateo, P. L., & Serrano, L. (1994) *Biochemistry 33*, 2142.
Weissman, J. S., & Kim, P. S. (1992) *Science 253*, 1386.
Wider, G., Neri, D., & Wüthrich, K. (1991) *J. Biomol. NMR 1*, 93.
Wishart, D. S., & Sykes, B. D. (1994) *Methods Enzymol. 239*, 363.
Wishart, D. S., Sykes, B. D., & Richards, F. M. (1991) *J. Mol. Biol. 222*, 311.
Wishart, D. S., Sykes, B. D., & Richards, F. M. (1992) *Biochemistry 31*, 1647.
Wishart, D. S., Bigam, C. G., Holm, A., Hodges, R. S., & Sykes, B. D. (1995) *J. Biomol. NMR 5*, 67.
Wittekind, M., Mapelli, C., Farmer, B. T., Suen, K.-L., Goldfarb, V., Tsao, J., Lavoie, T., Barbacid, M., Meyers, C., & Mueller, L. (1994) *Biochemistry 33*, 13531.
Wüthrich, K. (1986) *NMR of Proteins & Nucleic Acids*, Wiley, New York.
Yang, Y. S., Garbay, C., Duchesne, M., Cornille, F., Jullian, N., Fromage, N., Tocque, B., & Roques, B. P. (1994) *EMBO J. 13*, 1270.
Yu, H., Rosen, M. K., Shin. T. B., Siedel-Dugan, C., Brugge, J. S., & Schreiber, S. L. (1992) *Science 258*, 1665.
Yu, H., Chen, J. K., Feng, S., Dalgarno, D. C., Brauer, A. W., & Schreiber, S. L. (1994) *Cell 76*, 933.
Zhang, O., Kay, L. E., Olivier, J. P., & Forman-Kay, J. D. (1994) *J. Biomol. NMR 4*, 845.

BI942972N